Radiotherapy and Oncology 136 (2019) 161–168

Contents lists available at ScienceDirect

Radiotherapy and Oncology

journal homepage: www.thegreenjournal.com

Original Article

Setup strategies and uncertainties in esophageal radiotherapy based on detailed intra- and interfractional tumor motion mapping

Lone Hoffmann [a,*], Per R. Poulsen [b,c], Thomas Ravkilde [a], Jenny Bertholet [d], Iryna Kruhlikava [e], Bjørn L. Helbo [f], Mai L. Schmidt [a], Marianne Nordsmark [b]

[a] Aarhus University Hospital, Section for Medical Physics; [b] Aarhus University Hospital, Department of Oncology; [c] Aarhus University Hospital, Danish Centre for Particle Therapy, Denmark; [d] Joint Department of Physics, the Institute of Cancer Research and the Royal Marsden NHS Foundation Trust, London, UK; [e] Aarhus University Hospital, Department of Surgery; and [f] Aarhus University, Institute of Physics and Astronomy, Denmark

ARTICLE INFO

Article history:
Received 23 January 2019
Received in revised form 5 April 2019
Accepted 7 April 2019
Available online 20 April 2019

Keywords:
Esophageal cancer
Intrafractional motion
Interfractional motion
Fiducial markers
Soft tissue match

ABSTRACT

Background and purpose: Detailed knowledge of target motion is important for improved accuracy and decreased toxicity of esophageal cancer radiotherapy. This study uses the 3D trajectories of implanted markers during setup CBCT scans to investigate the intra- and interfractional tumor motion in esophageal cancer radiotherapy.

Material and methods: For 21 esophageal cancer patients with implanted fiducial markers, 60-s 3D marker trajectories were estimated from the 2D marker positions in the projections of daily setup CBCT scans by a probability-based method. The motion was separated into respiratory and cardiac components by frequency analysis and motion magnitude (2nd–98th percentile) was extracted for each marker. The mean motion was calculated over all markers. The daily mean setup interfraction error for bony-anatomy and soft-tissue setup was used to estimate the margin accounting for interfractional motion.

Results: A total of 1036 marker trajectories were extracted using 427 CBCT scans and 63 markers. The mean motion magnitude over all markers was 2.9 mm (left–right (LR)), 8.8 mm (cranio-caudal (CC)) and 4.1 mm (anterior–posterior (AP)) for the full motion during CBCT acquisition with mean magnitudes of 2.7 mm (LR), 8.4 mm (CC) and 3.5 mm (AP) for respiratory motion and 1.0 mm (LR), 1.5 mm (CC) and 1.4 mm (AP) for cardiac motion. Substantial daily marker shifts relative to bones resulted in margins of 8.9 mm (LR), 9.5 mm (CC), and 7.3 mm (AP). Soft-tissue based setup in and near the CTV combined with rescanning of patients with anatomical changes reduced the margins to 6.9 mm (LR), 6.8 mm (CC), and 5.6 mm (AP).

Conclusions: Esophageal tumor motion was mapped with unprecedented detail throughout the radiotherapy course. Respiratory motion dominated and was largest in the CC direction. Soft-tissue matching and an adaptive strategy reduced interfractional margins by 2–3 mm compared to bony-anatomy matching.

Discouraging overall survival rates have been the reality for esophageal cancer patients, although multimodality treatment combining chemo-radiotherapy (RT) with surgery has lately significantly increased the survival rate [1–4]. Large target volumes are often irradiated due to extensive tumor burden, the risk of subclinical spread along the esophagus and involvement of regional lymph nodes [5–6]. This results in increased risk of severe, potentially lethal normal tissue toxicities for the esophagus, heart and lungs [7–11]. This risk may be reduced by use of intensity modulated RT (IMRT) but cannot be eliminated entirely [12]. Tight margins and a smaller irradiated volume are needed to reduce the toxicity.

Esophageal tumors are typically large and complex in shape and the position of the target can change significantly between planning and treatment delivery [13–20]. Esophageal tumor motion relative to bony anatomy has previously been studied on an interfractional time scale based on tumor delineation on repetitive CT, Cone-Beam CT (CBCT) or Magnetic Resonance Imaging (MRI) scans [14,16,18–19] or marker segmentation in ten static 2D kV images or 7–8 CBCT images [15,20]. The largest shifts were seen in the cranio-caudal (CC) direction and for the most distal tumors. Lung and liver tumors have also been observed to move relative to the spinal cord and soft-tissue matching improved the setup accuracy [21–22]. Therefore, soft-tissue tumor-match may be more accurate

* Corresponding author at: Aarhus University Hospital, Department of Medical Physics, Noerrebrogade 44, Building 5J, 2. Floor, 8000 Aarhus C, Denmark.
E-mail address: Lone.Hoffmann@aarhus.rm.dk (L. Hoffmann).

https://doi.org/10.1016/j.radonc.2019.04.014
0167-8140/

than bony-anatomy based setup for esophageal cancer radiotherapy.

Respiration additionally results in intrafractional tumor motion, which has been studied by 20–60 s cine-MRI sequences acquired before [23–24] or a few times during [25] the treatment course. Fiducial markers implanted into the target have also been used to study motion in 4DCT [26–29] or 4D CBCT scans [30]. It provides the tumor position in typically ten phases during a single respiration cycle (4DCT) or averaged over an acquisition time of a few minutes (4DCBCT). However, respiratory cycles may vary considerably [31–32] and respiratory-induced motion described by 4DCT or 4DCBCT thus paints an incomplete picture.

A detailed 3D motion trajectory with resolution of the individual respiratory cycles can be obtained from fiducial markers through their 2D-trajectory in the projection images of a CBCT scan [33]. It can provide both respiratory and cardiac motion during the CBCT acquisition as previously shown for mediastinal lymph nodes [34].

In this study, we used implanted gold markers and the 3D trajectory-estimation method to investigate esophagus motion throughout the full treatment course in twenty-one esophageal cancer patients on both inter- and intrafractional time scales. Matching strategies for daily setup and margins were investigated as well as intrafractional motion magnitudes.

Material and methods

Patient data, treatment planning and delivery

Twenty-one patients with esophageal or gastro-esophageal junction (GEJ) cancer treated with chemo-RT between April 2016 and April 2017 were included in this study. All patients gave written informed consent and the study was approved by the Danish ethics committee. The cohort consisted of 6 females and 15 males with a median [range] age of 65 years [56–76 years].

The patients were planned and treated on a thorax-board (QFix, US) with their arms above the head. The gross tumor volume (GTV-T) and malignant lymph nodes (GTV-N) were delineated on the mid-ventilation phase selected by visual inspection of a planning 4DCT (pCT) scan with 3 mm slice thickness and guidance from a free-breathing ^{18}F-FDG-PET scan. The clinical target volume for the tumor (CTV-T) was created by adding 0.5 cm anterior–posterior (AP) and left–right (LR) margins and 3 cm cranio-caudal (CC) margins along the esophagus. The CTV for the lymph nodes (CTV-N) was created by adding isotropic 1 cm margins. The treated CTV was the union of CTV-T and CTV-N. The planning target volume (PTV) margin was 0.8 cm AP and LR and 1.1 cm CC. Patients were planned with IMRT delivering a homogeneous PTV dose of 50 Gy in 27 fractions (2 patients) or 41.4 Gy in 23 fractions (19 patients). All patients had Carboplatin and Paclitaxel concomitant with radiotherapy.

Daily patient setup was based on CBCT imaging with bony-anatomy match. An adaptive decision support protocol based on geometrical measures was used [13], requiring plan-adaptation when target deviations exceeded 0.5 cm for three consecutive fractions, as measured on the CBCT images. For the daily evaluation, the structure CTV + 5 mm was created and for each CT/CBCT slice, the radiation therapists evaluated if the CTV was inside this structure. Similarly, adaptation was performed if deviations in the diaphragm position exceeded 1 cm.

Marker implantation and location

Fiducial markers [0.5 mm × 5 mm Visicoil (IBA Dosimetry, Germany) or 0.28 mm × 20 mm Gold-Anchor (Naslund Medical AB, Sweden)] were implanted using ultrasound-guided endoscopy. The markers were implanted in the tumor submucosal layers at the center, cranial and caudal border of the GTV-T. The markers were classified into four anatomical sub-groups from proximal esophagus to proximal stomach based on their position according to the American Joint Committee on Cancer manual [35].

Imaging and image analysis

Each setup CBCT acquisition included ~670 kV projections acquired at 11 Hz during a full 60-s gantry rotation. The projections of 62 CBCT scans (12%) were lost from the data archive due to an unrecoverable hard drive failure. Each marker was segmented automatically in all CBCT projections that included the marker using a previously published method [36]. All segmentations were visually verified and manually corrected in case of segmentation errors. The resulting 2D marker-trajectory in the CBCT projections was used to estimate the 3D trajectory during the CBCT acquisition using a probability-based method [33,37]. Using frequency filters, the 2D-motion was automatically separated into motion inside and outside a 1–3 Hz frequency window, corresponding to cardiac-induced motion and non-cardiac motion (denoted respiratory motion), respectively. The transformation to 3D-motion was performed separately for the cardiac and respiratory motions, which were subsequently added to form the final combined 3D motion-trajectory.

Intrafraction motion

For each fraction, the motion magnitude (2nd–98th percentile) of each marker during the setup CBCT was determined for the cardiac, respiratory and combined motion from the 60 s 3D marker trajectories. For each marker, the mean motion magnitude over all fractions was calculated. The mean motion and standard deviation was calculated over all markers and over the markers in the four anatomical sub-groups.

Systematic respiration-induced elongation or contraction of the esophagus was investigated in 17 patients with more than one implanted marker as respiratory changes in the CC distance between the most cranial and most caudal marker. A fraction with regular respiratory motion throughout the CBCT scan was selected for these patients and the difference between the largest and smallest inter-marker distance (2nd–98th percentile) during the CBCT was reported.

Interfraction motion and margins

The mean position of each marker at each fraction was determined from their combined 3D trajectories and used to calculate the interfractional margins in three setup scenarios. First, the daily mean setup error relative to the bony-anatomy at pCT was calculated for each marker and all fractions taking into account the couch shift applied between setup CBCT and treatment delivery based on bony-anatomy matching. It gives the setup error caused by internal tumor shifts relative to the original patient anatomy. Second, 12 patients had one or two rescans and plan-adaptations during the treatment course and the mean setup error relative to the CT scan currently in use (denoted actual CT) was calculated. It gives the actual setup error in the applied adaptive protocol. Third, the mean setup error for each marker was determined relative to an automatic offline soft-tissue match based on tissue in and near the CTV using the actual CT scan. The rigid registration software Offline Review (Varian Medical Systems, CA) was used for the match. This gives the setup error at the position of the markers when a soft-tissue setup protocol is used. A clipbox encompassing the CTV plus 1 cm isotropically was used for the match. After each automatic soft-tissue registration, a visual

inspection of the alignment of the CBCT scans was performed. The grand mean (M) and standard deviations of the systematic ($\sum$) and random (σ) errors were calculated for each of the three scenarios using all markers in combination as well as markers divided into each of the four sub-groups. The daily mean setup error was used to estimate the margin required to deliver at least 95% dose to the CTV in 90% of the patients as

$$2.5\sum + 1.64\sqrt{\sigma^2 + \left(\frac{A}{3}\right)^2 + \sigma_p^2} - \sigma_p^2$$

for all markers and for the four sub-groups of markers [38]. σ_p characterizes the penumbra width and was set to 3 mm. A is the peak-to-peak amplitude of the intrafraction marker motion, which includes both respiratory and cardiac motion. The margin was calculated with $A = 0$ (not accounting for intrafraction motion) and A equal to the mean intrafraction motion range as measured on the CBCT projections. All other uncertainties were neglected.

Statistics

The interfractional displacements in LR, CC and AP direction between bony anatomy setup on pCT and soft tissue setup on actual CT was assessed using the Wilcoxon signed-rank test. $p < 0.05$ was considered statistically significant. Likewise, the motion amplitude on 4DCT was compared to the motion amplitude on CBCT in LR, CC and AP direction.

Results

The median [range] GTV-T, GTV-N and CTV volumes were 33.7 cm^3 [10.2–96.6 cm^3], 2.2 cm^3 [0–25.6 cm^3] and 246.8 cm^3 [107.5–404.0 cm^3], respectively. Twelve patients had one or two rescans during the treatment course due to systematic anatomical changes ($n = 8$) or changes in the position of the diaphragm ($n = 4$). Full patient characteristic is given in Supplementary Table 1.

In six patients, two additional markers were implanted 2 cm cranial and caudal to the GTV-T. This resulted in a total of 29 Visicoil and 43 Gold-Anchor markers with 2–7 markers in each patient. At pCT, 27 Visicoil markers (93%) and 38 Gold-Anchor markers (88%) were seen. At the first fraction, two more Gold-Anchor markers were missing. No markers were lost during the treatment course. Some markers were not segmented due to poor contrast or close vicinity to other segmented markers. In total, 49 markers were segmented. The markers were grouped according to the proximal ($n = 5$), middle ($n = 11$) and distal ($n = 26$) esophagus and the proximal stomach ($n = 7$). A total of 1036 marker trajectories were extracted in 427 CBCT scans. The median [range] number of segmented fractions per patient was 22 [6–27]. For further details, see Supplementary Table 1.

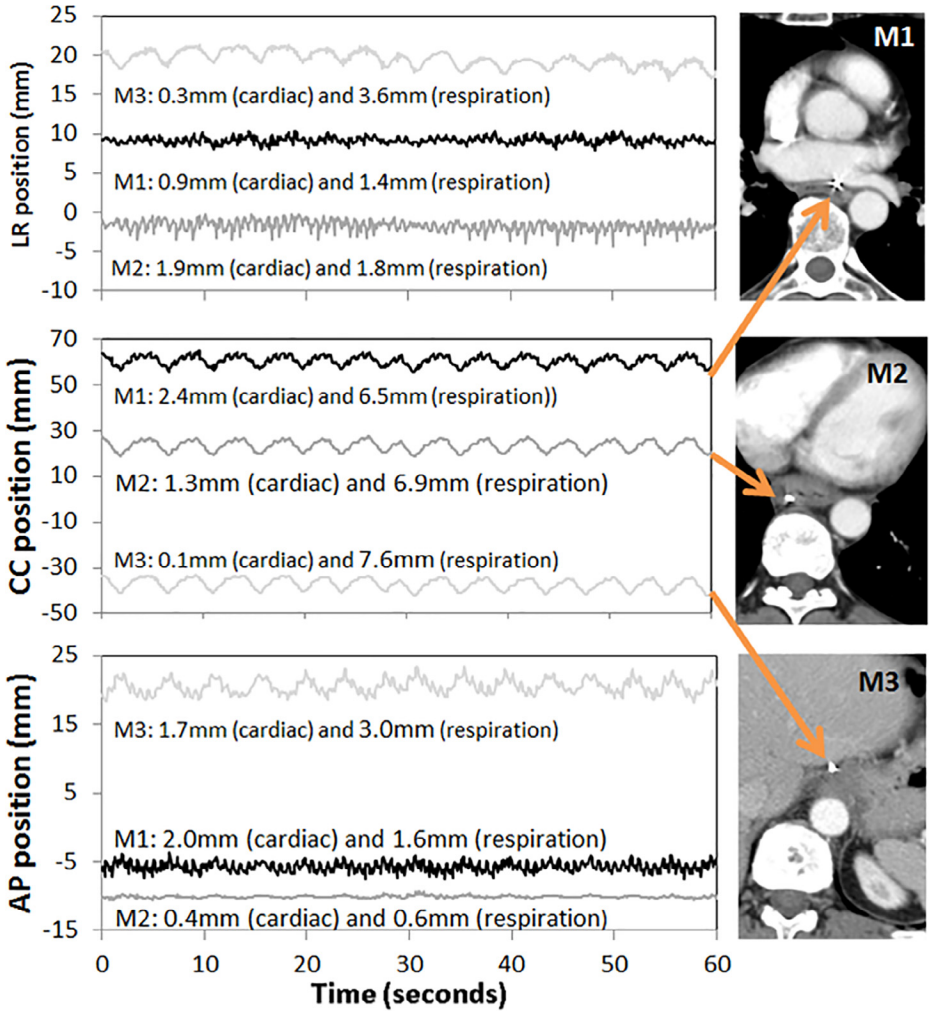

Fig. 1. Intrafractional motion of three markers during the CBCT at fraction 9 of a patient. The anatomical positions of the markers (M) are shown to the right. M1 is located in the middle esophagus, M2 in the distal esophagus and M3 in the proximal stomach. All positions are relative to the isocenter after bony anatomy alignment. All motion ranges are 2nd–98th percentile ranges.

Fig. 1 shows the intrafractional motion at one fraction for a patient with three markers implanted. The CC motion was dominated by respiration and nearly identical for all markers, while the LR and AP respiratory motion and the cardiac motion in all directions varied more among the markers. The mean and standard deviation of the 2nd–98th percentile motion amplitude during 60-s CBCT acquisition is shown in Table 1 for the full motion and for the respiratory and cardiac motion components. Furthermore, the motion during the 4D pCT is shown and it is significantly ($p < 0.001$) smaller than at treatment in all three directions. The respiratory motion was largest in the CC-direction and for markers in the distal esophagus or the proximal stomach, where the motion in the AP-direction was also substantial. Cardiac-induced motion was small and exceeded 2 mm in at least one direction for 20 markers (41%).

The motion varied both intra- and interfractionally, as exemplified in Fig. 2 for marker M1 in the patient presented in Fig. 1. At fraction 3, an otherwise regular respiratory curve presented a few large cranial excursions. At fraction 6, the marker had moved medially into a stable position with nearly no motion, especially in the AP-direction. The marker switched back to the lateral position at fraction 12 restoring the regular motion. In fraction 18 (and 19, not shown), irregular motion with low respiratory frequency was seen. Finally, at the end of the treatment course, the motion was regular with low amplitude in all three directions. The variability in intra- and interfractional motion magnitudes differed among the patients with some showing stable and reproducible motion magnitudes and others exhibiting high variability.

The median CC distance between the most cranial and most caudal marker was 44.5 mm (range 22.3–149.3 mm). The median magnitude of the respiration-induced inter-marker distance changes was 2.7 mm (range 1.2–6.4 mm). The inter-marker distance was largest at inhale at all fractions for eight patients, at exhale for five patients, midway between inhale and exhale for two patients, while the phase with largest inter-marker distance changed interfractionally between inhale and exhale for two patients. No systematic trend in terms of esophagus elongation or contraction at a specific breathing cycle was seen in the inter-marker motion for the patient cohort.

Fig. 3 shows the interfractional motion for a patient with four markers implanted. A 9 mm lateral shift occurred between fraction 3 and fraction 5 for the most cranial marker (M1). An abrupt lateral

Table 1
Mean (standard deviation) of the intrafraction motion magnitude during 4DCT and CBCT acquisition.

	Total motion 4DCT (mm)				Total motion CBCT (mm)			Respiratory motion CBCT (mm)			Cardiac motion CBCT (mm)		
	N	LR	CC	AP	LR	CC	AP	LR	CC	AP	LR	CC	AP
All markers	49	1.8 (1.6)	6.8 (4.0)	2.9 (3.2)	2.9 (1.4)	8.8 (2.9)	4.1 (2.7)	2.7 (1.3)	8.4 (2.8)	3.5 (2.6)	1.0 (0.5)	1.5 (0.6)	1.4 (0.6)
Proximal E	5	0.7 (0.7)	3.8 (3.2)	1.4 (0.5)	1.8 (0.6)	6.5 (2.4)	2.1 (0.5)	1.6 (0.5)	6.4 (2.3)	1.8 (0.5)	0.6 (0.2)	1.1 (0.5)	0.9 (0.4)
Middle E	11	1.8 (2.1)	4.3 (2.5)	1.1 (0.7)	2.6 (1.1)	6.7 (2.6)	2.3 (0.9)	2.3 (1.0)	6.3 (2.5)	1.7 (0.9)	1.0 (0.4)	1.3 (0.6)	1.3 (0.5)
Distal E	26	2.0 (1.6)	7.6 (3.8)	3.1 (3.2)	3.3 (1.5)	9.8 (2.6)	4.5 (2.8)	2.9 (1.4)	9.3 (2.5)	4.0 (2.8)	1.2 (0.7)	1.8 (0.6)	1.5 (0.7)
Proximal S	7	2.1 (1.2)	9.7 (4.4)	5.9 (4.6)	3.2 (1.6)	9.8 (2.3)	6.4 (2.3)	3.3 (1.6)	9.8 (2.4)	6.1 (2.6)	0.5 (0.2)	1.5 (0.4)	1.6 (0.3)

Abbreviations: N = number of markers, E = esophagus, S = stomach, LR = left–right, CC = cranio-caudal, AP = anterior–posterior.

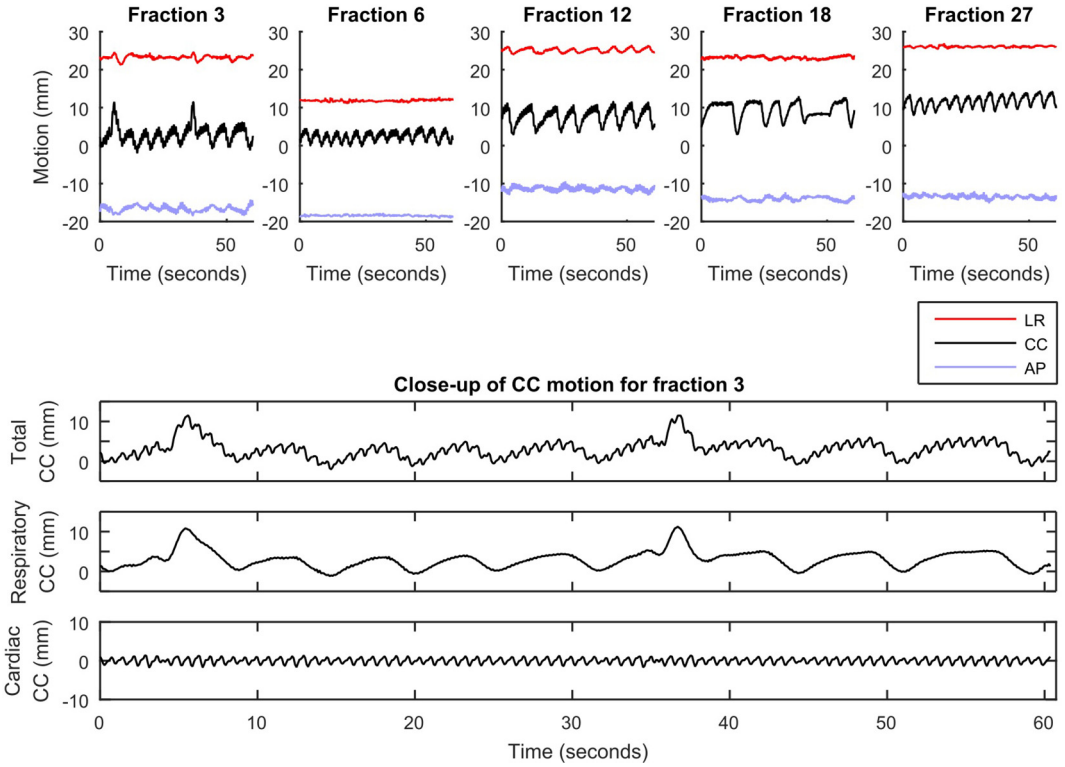

Fig. 2. Examples of motion trajectories for marker M1 (see Fig. 1 for anatomical position of marker). Top panel: Motion trajectories in left–right (LR), cranio-caudal (CC) and anterio-posterior (AP) directions during selected fractions. Bottom panel: Close-up of CC motion during fraction 3. The motion (total) is split into respiratory and cardiac components.

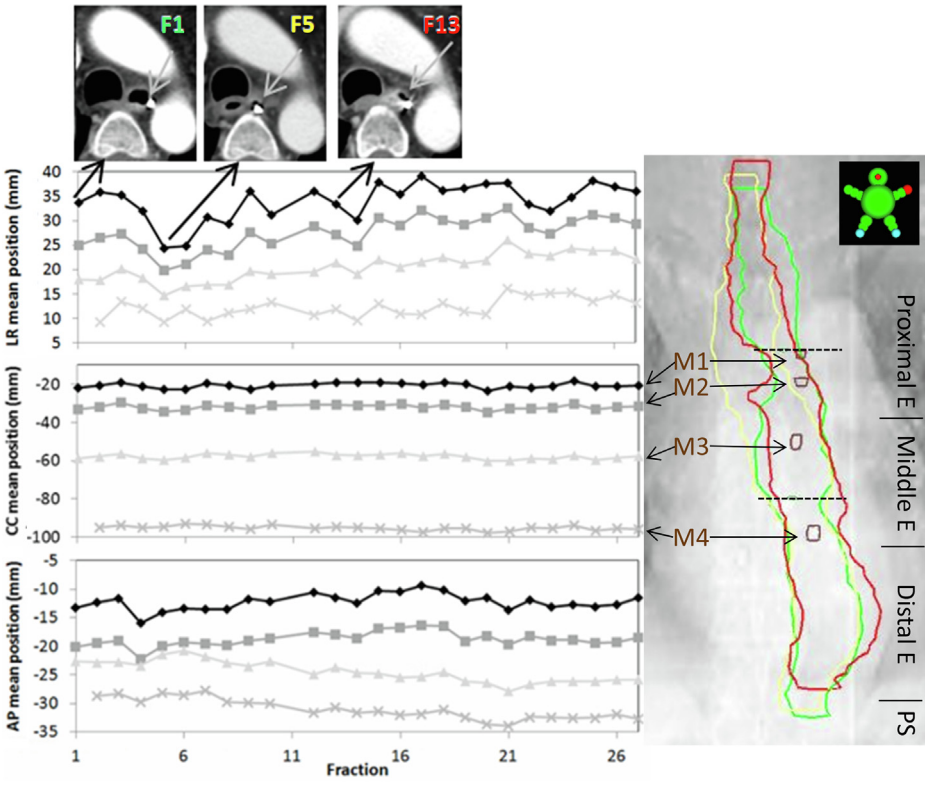

Fig. 3. Interfractional motion of four markers during 27 fractions for a patient in the left–right (LR), cranio-caudal (CC) and anterio-posterior (AP) directions. Upper: the position of M1 at fractions 1, 5 and 13. Below-left: All positions are relative to the isocenter after bony anatomy alignment. However, in the LR direction the position of M1 was shifted by 10 mm, M3 by −5mm and M4 by −20 mm in order to separate the curves. Right: Topographic representation of the delineated esophagus in each of the three CT scans used for fractions 1, 5 and 13, respectively. The positions of the markers at fraction 1 are shown as contours at the tips of the arrows. The cranial and caudal extent of the GTV-T is marked by dashed lines. Solid lines mark the anatomical borders between regions defined by the American Joint Committee on Cancer manual [35] used for dividing the markers into the four sub-groups.

Table 2
Interfraction shifts for 49 markers after matching on (1) bones using pCT, (2) bones using actual CT or 3) CTV using soft-tissue matching.

	All markers (mm)			Proximal E (mm)			Middle E (mm)			Distal E (mm)			Proximal S (mm)		
	LR	CC	AP	LR	CC	AP	LR	CC	AP	LR	CC	AP	LR	CC	AP
N		49			5			11			26			7	
Bony-anatomy match using pCT															
GM	0.8	2.0	0.0	−0.9	3.8	1.0	0.1	1.0	−0.4	1.8	2.1	0.3	−0.8	2.2	−1.3
∑	2.9	3.1	2.5	2.4	3.1	1.1	2.1	2.2	1.1	2.9	3.5	1.6	3.3	2.4	5.6
σ	2.4	2.5	1.6	2.4	1.7	1.7	1.7	1.6	1.2	2.6	2.8	1.5	2.5	2.7	2.2
Margin (A = 0)	8.6	9.2	6.8	7.5	8.4	3.6	6.0	6.2	3.2	9.0	10.5	4.6	9.8	7.6	15.2
Margin (A = Amean)	8.8	10.8	7.2	7.6	9.5	3.7	6.2	7.2	3.4	9.2	12.3	5.1	10.0	9.7	16.3
Bony-anatomy match using actual CT															
GM	0.5	1.3	0.0	0.8	1.9	0.6	0.3	0.8	−0.2	0.8	1.3	0.3	−1.2	1.8	−0.7
∑	2.1	2.5	1.8	1.4	1.7	1.0	1.9	1.7	1.1	2.1	3.0	1.4	2.5	2.4	3.9
σ	2.6	2.7	1.9	3.3	2.3	1.9	1.6	1.9	1.2	2.5	3.0	1.8	3.2	2.8	3.1
Margin (A = 0)	6.9	7.9	5.5	6.4	5.5	3.3	5.4	5.2	3.1	6.7	9.5	4.3	8.5	7.8	11.8
Margin (A = Amean)	7.1	9.5	5.9	6.4	6.5	5.5	5.5	6.2	3.3	7.0	11.4	4.8	8.7	9.9	12.7
Soft-tissue match															
GM	0.9	1.9	−0.1	1.2	2.3	0.9	0.7	1.1	0.0	1.3	2.1	−0.1	−0.6	2.7	−0.8
∑	2.1	2.1	1.7	1.1	1.7	1.1	1.9	1.5	1.3	2.1	2.3	1.4	2.3	2.2	3.4
σ	2.3	2.4	1.9	2.9	2.0	2.0	1.4	1.6	1.2	2.3	2.5	1.7	2.9	2.6	2.8
Margin (A = 0)	6.6	6.5	5.2	4.8	5.2	3.7	5.2	4.4	3.6	6.6	7.2	4.2	7.6	7.2	10.5
Margin (A = Amean)	6.8	8.2	5.6	4.9	5.3	3.8	5.4	5.4	3.7	6.9	9.1	4.7	7.9	9.4	11.5

Abbreviations: N = number of markers, LR = left–right, CC = cranio-caudal, AP = anterior–posterior, E = esophagus, S = stomach. GM = grand mean, Σ = systematic error, σ = random error. Amean = mean amplitude of intrafraction margin

shift of the esophagus resulted in this marker shift. Only minor shifts occurred for the more caudal markers as well as the nearby esophageal tissue. Esophageal lateral shifts of varying size were observed throughout the treatment course for this patient, while the AP and CC positions were more stable. Daily marker-shifts relative to bones were in general quite large for the patient cohort as shown in Table 2 together with the interfraction motion margins. The margins depend on the anatomical position of the tumor and

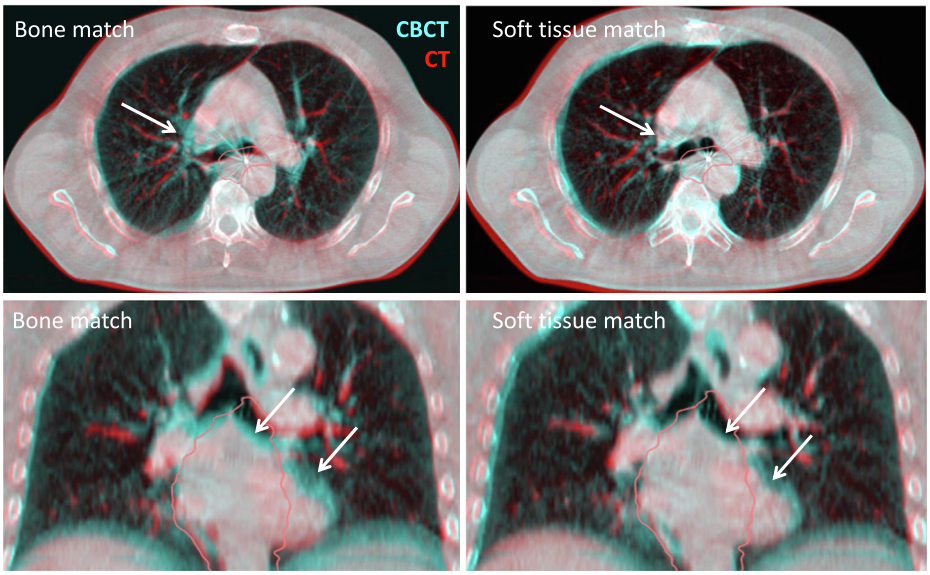

Fig. 4. Overlay of CT and CBCT shown together with CTV delineated in the CT scan. Left: After bony-anatomy match, where CC-deviations are seen in the mediastinum. Right: After soft tissue match on the CTV, the deviations have been removed and a perfect match is seen. Arrows mark anatomical deviations appearing after bony-anatomy matching.

are small for the middle esophagus and large for the proximal stomach especially in the AP-direction as compared to the other sub-groups. Setup based on rescanning for patients with anatomical changes during the RT course allowed margin reduction in all directions for all sub-groups. Soft-tissue matching allowed further margin reduction especially in the CC direction giving an overall reduction of 2–3 mm in all directions for soft-tissue setup compared to bony anatomy setup using the pCT scan. In all sub-groups, soft-tissue matches combined with rescanning of patients with anatomical changes according to the adaptive protocol lead to smaller or similar margins as for bone matches. In the proximal stomach region, a margin reduction of 5 mm in AP-direction was seen (Table 2). However, for these abdominal tumors large inter-fraction mobility was seen and the margins ranged from 7 mm (CC) to 11 mm (AP) even after soft-tissue matching (see Suppl. Fig. 1). For proximal and middle esophageal tumors, margins of 4–5 mm were found with the smallest margin in the AP direction.

A comparison of bone and soft-tissue matching is shown in Fig. 4. The bone match resulted in a 5 mm cranial error of the marker and the CTV, which was resolved by soft-tissue matching.

The absolute systematic errors of all markers were not significantly different ($p = 0.477$ (LR), $p = 0.276$ (CC), $p = 0.724$ (AP)) between bone match using pCT and soft-tissue match. However, the standard deviations of the errors in the LR and AP directions were significantly larger ($p = 0.024$ and $p = 0.038$, respectively) for the bone match on pCT. No testing was performed for the sub-groups due to the limited number of patients.

Inclusion of the intrafraction motion in the margin calculation resulted in only slight increase of 2–4 mm in the LR and AP direction, whereas the margin in the CC direction increased by 1.7–8.2 mm for the full patient cohort (Table 2). The intrafraction motion should therefore be taken into account for the margin calculation.

Discussion

Twenty-one esophageal cancer patients had 72 markers implanted in or nearby their tumor. All patients had daily CBCT scans for bony-anatomy setup. The treatment strategy was based on an adaptive protocol triggering rescanning of patients with anatomical changes. Soft-tissue matching on the CTV was performed retrospectively and was found to allow margin reduction by 2–3 mm in combination with the adaptive strategy. We have thus changed to soft-tissue matching in our clinic. The intrafractional 3D motion of 49 markers was extracted from the projections of the daily CBCT scans (427 scans in total) with high temporal resolution (11 Hz) during 60-s acquisition. Hereby, intra- and inter-fractional data acquired from daily CBCT scans with much higher temporal resolution was available than in any former intrafractional studies based on one 4DCT scan [26,39] or one online pre-treatment cine-MRI [23–24]. Due to the high temporal resolution, the trajectories could be separated into cardiac and respiratory intrafraction motion.

The feasibility of endoscopic marker implantation in the submucosal layers of the esophagus was investigated in a former study comparing implantation of three different markers and 87.5% to 98% of the markers were visible at pCT [40]. In the current study, two marker types were used. At pCT, 93% Visicoil markers and 88% Gold-Anchor markers were visible. All Visicoils stayed visible during the full treatment course, while 7% Gold-Anchors were lost. However, 7% of the Visicoils and 16% of the Gold-Anchors were lost between implantation and start of the treatment course. In all 21 patients the implantation of gold markers was successfully and safely performed during standard gastroscopy by a specialized upper gastrointestinal surgeon.

The interfractional motion of esophageal tumors relative to the bony-anatomy has previously been reported [14–16,18–20]. Jin et al. [20] analyzed the interfractional shifts of 65 markers and found systematic/random errors of 2.9/2.4 mm (LR), 4.1/2.4 mm (CC) and 2.2/1.8 mm (AP), comparable to the findings in the present study. Furthermore, the largest motion was found for markers in the proximal stomach, in accordance with the current study. The daily marker-shifts relative to bones were large. A reduction in the marker-shifts was found by rescanning of patients with anatomical changes during the RT course and the margins were reduced by 1–2 mm compared to bony-anatomy setup using the pCT.

Daily soft-tissue matching based on the CTV reduced the inter-fraction variation for the markers even further. No testing was performed for the sub-groups due to the limited number of patients.

Deviations were still present due to the complex shape of the tumor precluding perfect matching. Automatic matching on soft-tissue could be error-prone due to low contrast in the mediastinum and below the GEJ. However, all matches were checked manually and no corrections were indicated showing high reliability in the match performed by the offline image-registration software. In a recent study, bony-anatomy setup was found to result in smaller margins than carina based setup [41]. As the CC length of the esophagus is 25–30 cm, the carina might be a poor position surrogate for very cranial or caudal esophageal tumors.

The margins for soft-tissue matching depend on the position of the tumor. For tumors located in the proximal or middle esophagus, margins of 4–6 mm were found. These margins increase to 5–7 mm for the distal esophagus. In proximal, middle and distal esophagus, the AP margin was smallest. For tumors in the proximal stomach, large margins of 7–11 mm were found with the largest margin in the AP-direction. In this abdominal region, the organ motion is large resulting in target deformations, which cannot be completely solved by soft-tissue matching (see Suppl. Fig. 1). The margins were calculated based on observed motion of markers implanted in the GTV-T, thus assuming that the markers reasonably represent the entirety of the CTV. The cranial or caudal part of the CTV may deform compared to the GTV. However, soft tissue registrations on GTV or CTV in three randomly selected patients deviated at maximum 1 mm in all cardinal directions.

In some patients, the inter-marker distance in one or more directions varied interfractionally due to slight anatomical changes, as exemplified in Fig. 3 and Suppl. Fig. 1. These changes were present in all regions of the esophagus and illustrate that the markers only represent small volumes of the deformable tumor. The anatomical changes may result from deformation, tumor growth or shrinkage [13,17].

To comply with the findings in this study, we have changed our clinical margins to 8 mm (LR), 11 mm (CC) and 8 mm (AP). These margins are larger than those stated in Table 2, as the margins also account for delineation uncertainties, intrafractional shifts not related to respiratory or cardiac motion, target deformation and motion relative to the markers, and machine uncertainties. The margins may be reduced using margins specific to the anatomical regions.

The margin calculation was based on a small number of markers in the proximal esophagus and in the proximal stomach and thus, the numbers include uncertainties. However, a large difference in interfractional motion between proximal/middle esophagus and proximal stomach was seen.

Baseline interfraction shifts of the markers between CT and the daily CBCT scans were observed in the cranial direction (GM = 2.0 mm in Table 2). Similar shifts have been observed for lung [42–43] and liver [44–45] patients. However, these shifts were seen intrafractionally during the treatment, showing anatomical changes for some time after positioning of the patient. A likely reason for the cranial shift could be the change of gravitational forces from caudal to posterior direction with supine patient positioning. The interfractional shifts could indicate differences in the time used for positioning at CT and accelerator. We can only speculate that the time used at the accelerator is longer than at CT, as we have no measurements available.

High temporal resolution was obtained for the intrafractional marker-motion. We found largest intrafractional motion in the distal esophagus and in the proximal stomach in accordance with previous results [23–28]. The motion was largest in the CC direction with a mean magnitude of 8.8 mm, which is comparable to previously published results [23,28,29]. Minor motion was seen in LR and AP, except for the proximal stomach where the mean AP motion was 6.1 mm, comparable to the results of Jin et al. and Zhao et al. [29,42]. In some patients, high variability in intra- and inter-fractional motion magnitude was seen, whereas others showed stable motion magnitudes. High variability was found in a study of 20 patients who underwent MRI six times during the treatment course showing large interfractional and inter-patient variability in motion magnitude [25]. On the contrary, low interfractional variability (mean $\leq$1.4 mm) was found in a study of 63 markers segmented in setup CBCT scans (median 8 scans) [30]. Also the intrafractional displacement of markers was found to be patient dependent and to differ up to 3 mm between markers implanted in the same tumor [26]. This indicates that patients could be separated into groups of either high or low motion variability, possibly allowing intensified monitoring of patients in the high motion variability category.

The 4DCT intrafraction motion amplitude was smaller than the motion amplitude at CBCT, possibly due to the fact that only one breathing cycle is captured during 4DCT, while the intrafraction motion amplitude during the 60-s CBCT scan is determined by the largest breathing motion in the measurement interval. Smaller 4DCT motion than CBCT has also been found for lung and liver [42,46] and the setup CBCT provides a better estimate of the intra-treatment motion than the 4DCT scan.

The intrafraction motion was separated into cardiac and respiratory motion. The respiratory-induced motion was most pronounced in CC-direction and for the most caudal markers, whereas the cardiac-induced motion was small with 41% of the markers experiencing motion >2 mm in at least one direction with a tendency for larger motion in the distal esophagus. Cardiac-induced motion of the esophagus has been studied by contrast-enhanced CT-based coronary angiography with electrocardiographic gating in non-cancer patients [47]. The mean esophageal motion varied from 1 to 3 mm, with the largest motion in the distal esophagus. Similarly, for lung tumors or mediastinal lymph nodes nearby the cardiac or aortic wall, cardiac-induced motion of 1–4 mm was seen [34,48].

In conclusion, detailed 3D intra- and interfractional motion of fiducial markers in esophageal cancer patients were obtained from daily CBCT projection images. The respiratory motion was largest in CC-direction, while cardiac motion was small and nearly identical in all directions. Large interfractional shifts correlated with positional changes of the esophagus were observed in some patients. Soft-tissue matching reduced interfractional margins by 2–3 mm compared to bony-anatomy matching.

Acknowledgements

Naslund Medical AB, Sweden is acknowledged for providing Gold Anchor fiducial markers.

The work was supported by the Danish Cancer Society, the Danish Comprehensive Cancer Center (grant R191-A11526) and Varian Medical Systems, Inc.

Conflict of interest statement

None.

Appendix A. Supplementary data

Supplementary data to this article can be found online at https://doi.org/10.1016/j.radonc.2019.04.014.

References

[1] Ng J, Lee P. The role of radiotherapy in localized esophageal and gastric cancer. Hematol Oncol Clin North Am 2017;31:453–68.

[2] So B, Marcu L, Olver I, Gowda R, Bezak E. Oesophageal cancer: Which treatment is the easiest to swallow? A review of combined modality treatments for resectable carcinomas. Crit Rev Oncol Hematol 2017;113:135–50.
[3] van Hagen P, Hulshof MC, van Lanschot JJ, Steyerberg EW, van Berge Henegouwen MI, Wijnhoven BP, et al. Preoperative chemoradiotherapy for esophageal or junctional cancer. N Engl J Med 2012;366:2074–84.
[4] Shapiro J, van Lanschot JJB, Hulshof MCCM, van Hagen P, van Berge Henegouwen MI, Wijnhoven BPL, et al. Neoadjuvant chemoradiotherapy plus surgery versus surgery alone for oesophageal or junctional cancer (CROSS): long-term results of a randomised controlled trial. Lancet Oncol 2015;16:1090–8.
[5] Wu AJ, Bosch WR, Chang DT, Hong TS, Jabbour SK, Kleinberg LR, et al. Expert consensus contouring guidelines for IMRT in esophageal and gastroesophageal junction cancer. Int J Radiat Oncol Biol Phys 2015;92:911–20.
[6] Tachimori Y. Pattern of lymph node metastases of squamous cell esophageal cancer based on the anatomical lymphatic drainage system: efficacy of lymph node dissection according to tumor location. J Thorac Dis 2017;9:S724–30.
[7] Lee HK, Vaporciyan AA, Cox JD, Tucker SL, Putnam Jr JB, Ajani JA, et al. Postoperative pulmonary complications after preoperative chemoradiation for esophageal carcinoma: Correlation with pulmonary dose-volume histogram parameters. Int J Radiat Oncol Biol Phys 2003;57:1317–22.
[8] Shirai K, Tamaki Y, Kitamoto Y, Murata K, Satoh Y, Higuchi K, et al. Dose-volume histogram parameters and clinical factors associated with pleural effusion after chemoradiotherapy in esophageal cancer patients. Int J Radiat Oncol Biol Phys 2011;80:10021097.
[9] Beukema JC, van Luijk P, Widder J, Langendijk JA, Muijs CT. Is cardiac toxicity a relevant issue in the radiation treatment of esophageal cancer? Radiother Oncol 2015;114:85–90.
[10] Accordino MK, Neugut AI, Hershman DL. Cardiac effects of anticancer therapy in the elderly. J Clin Oncol 2014;32:2654–61.
[11] Wang J, Wei C, Tucker SL, Myles B, Palmer M, Hofstetter WL, et al. Predictors of postoperative complications after trimodality therapy for esophageal cancer. Int J Radiat Oncol Biol Phys 2013;86:885–91.
[12] Kole TP, Aghayere O, Kwah J, Yorke ED, Goodman KA. Comparison of heart and coronary artery doses associated with intensity-modulated radiotherapy versus three-dimensional conformal radiotherapy for distal esophageal cancer. Int J Radiat Oncol Biol Phys 2012;83:1580–6.
[13] Nyeng TB, Nordsmark M, Hoffmann L. Dosimetric evaluation of anatomical changes during treatment to identify criteria for adaptive radiotherapy in oesophageal cancer patients. Acta Oncol 2015;54:1467–73.
[14] Cardenas ML, Mazur TR, Tsien CI, Green OL. A rapid, computational approach for assessing interfraction esophageal motion for use in stereotactic body radiation therapy planning. Adv Radiat Oncol 2017;3:209–15.
[15] Fukada J, Hanada T, Kawaguchi O, Ohashi T, Takeuchi H, Kitagawa Y, et al. Detection of esophageal fiducial marker displacement during radiation therapy with a 2-dimensional on-board imager: analysis of internal margin for esophageal cancer. Int J Radiat Oncol Biol Phys 2013;85:991–8.
[16] Wang JZ, Li JB, Wang W, Qi HP, Ma ZF, Zhang YJ, et al. Detection of interfraction displacement and volume variance during radiotherapy of primary thoracic esophageal cancer based on repeated four-dimensional CT scans. Radiat Oncol 2013;8:224.
[17] Wang JZ, Li JB, Wang W, Qi HP, Ma ZF, Zhang YJ, et al. Changes in tumour volume and motion during radiotherapy for thoracic oesophageal cancer. Radiother Oncol 2015;114:201–5.
[18] Yamashita H, Haga A, Hayakawa Y, Okuma K, Yoda K, Okano Y, et al. Patient setup error and day-to-day esophageal motion error analyzed by cone-beam computed tomography in radiation therapy. Acta Oncol 2010;49:485–90.
[19] Cohen RJ, Paskalev K, Litwin S, Price Jr RA, Feigenberg SJ, Konski AA. Esophageal motion during radiotherapy: quantification and margin implications. Dis Esophagus 2010;23:473–9.
[20] Jin P, van der Horst A, de Jong R, van Hooft JE, Kamphuis M, van Wieringen N, et al. Marker-based quantification of interfractional tumor position variation and the use of markers for setup verification in radiation therapy for esophageal cancer. Radiother Oncol 2015;117:412–8.
[21] Hoffmann L, Holt MI, Knap MM, Khalil AA, Møller DS. Anatomical landmarks accurately determine interfractional lymph node shifts during radiotherapy of lung cancer patients. Radiother Oncol 2017;116:64–9.
[22] Bertholet J, Worm E, Høyer M, Poulsen P. Cone beam CT-based set-up strategies with and without rotational correction for stereotactic body radiation therapy in the liver. Acta Oncol 2017;56:860–6.
[23] Lever FM, Lips IM, Crijns SP, Reerink O, van Lier AL, Moerland MA, et al. Quantification of esophageal tumor motion on cine-magnetic resonance imaging. Int J Radiat Oncol Biol Phys 2014;88:419–24.
[24] Zhou HY, Zhang JG, Li R, Zhang XM, Chen TW, Liu N, et al. Tumour motion of oesophageal squamous cell carcinoma evaluated by cine MRI: associated with tumour location. Clin Radiol 2018;73:676.e1–7.
[25] Heethuis SE, Borggreve AS, Goense L, van Rossum PSN, Mook S, van Hillegersberg R, et al. Quantification of variations in intra-fraction motion of esophageal tumors over the course of neoadjuvant chemoradiotherapy based on cine-MRI. Phys Med Biol 2018;63:145019.
[26] Liu F, Ng S, Huguet F, Yorke ED, Mageras GS, Goodman KA. Are fiducial markers useful surrogates when using respiratory gating to reduce motion of gastroesophageal junction tumors? Acta Oncol 2016;55:1040–6.
[27] Doi Y, Murakami Y, Imano N, Takeuchi Y, Takahashi I, Nishibuchi I, et al. Quantifying esophageal motion during freebreathing and breath-hold using fiducial markers in patients with early-stage esophageal cancer. PLoS ONE 2018;13:e0198844.
[28] Yamashita H, Kida S, Sakumi A, Haga A, Ito S, Onoe T, et al. Four-dimensional measurement of the displacement of internal fiducial markers during 320-multislice computed tomography scanning of thoracic esophageal cancer. Int J Radiat Oncol Biol Phys 2011;79:588–95.
[29] Jin P, Hulshof MC, de Jong R, van Hooft JE, Bel A, Alderliesten T. Quantification of respiration-induced esophageal tumor motion using fiducial markers and four-dimensional computed tomography. Radiother Oncol 2016;118:492–7.
[30] Jin P, Hulshof MCCM, van Wieringen N, Bel A, Alderliesten T. Interfractional variability of respiration-induced esophageal tumor motion quantified using fiducial markers and four-dimensional cone-beam computed tomography. Radiother Oncol 2017;124:147–54.
[31] Korreman SS. Image-guided radiotherapy and motion management in lung cancer. Br J Radiol 2015;88:20150100.
[32] Keall PJ, Mageras GS, Balter JM, Emery RS, Forster KM, Jiang SB, et al. The management of respiratory motion in radiation oncology report of AAPM Task Group 76. Med Phys 2006;33:3874–900.
[33] Poulsen PR, Cho B, Keall PJ. A method to estimate mean position, motion magnitude, motion correlation, and trajectory of a tumor from cone-beam CT projections for image-guided radiotherapy. Int J Rad Onc Biol Phys 2008;72:1587–96.
[34] Schmidt ML, Hoffmann L, Knap MM, Rasmussen TR, Folkersen BH, Toftegaard J, et al. Cardiac and respiration induced motion of mediastinal lymph node targets in lung cancer patients throughout the radiotherapy treatment course. Radiother Oncol 2016;121:52–8.
[35] Rice TW, Blackstone EH, Rusch VW. 7th Edition of the AJCC Cancer Staging Manual: esophagus and esophagogastric junction. Ann Surg Oncol 2010;17:1721–4.
[36] Bertholet J, Wan H, Toftegaard J, Schmidt ML, Chotard F, Parikh PJ, et al. Fully automatic segmentation of arbitrarily shaped fiducial markers in CBCT projections. Phys Med Biol 2017;62:1327–41.
[37] Poulsen PR, Cho B, Keall PJ. Real-time prostate trajectory estimation with a single imager in arc radiotherapy: a simulation study. Phys Med Biol 2009;54:4019–35.
[38] van Herk M. Errors and margins in radiotherapy. Semin Radiat Oncol 2004;14:52–64.
[39] Dieleman EM, Senan S, Vincent A, Lagerwaard FJ, Slotman BJ, van Sörnsen, et al. Four-dimensional computed tomographic analysis of esophageal mobility during normal respiration. Int J Radiat Oncol Biol Phys 2007;67:775–80.
[40] Machiels M, van Hooft J, Jin P, van Berge Henegouwen MI, van Laarhoven HM, Alderliesten T, et al. Endoscopy/EUS-guided fiducial marker placement in patients with esophageal cancer: a comparative analysis of 3 types of markers. Gastrointest Endosc 2015;82:641–9.
[41] Machiels M, Jin P, van Gurp CH, van Hooft JE, Alderliesten T, Hulshof MCCM. Comparison of carina-based versus bony anatomy-based registration for setup verification in esophageal cancer radiotherapy. Radiat Oncol 2018;13:48.
[42] Schmidt ML, Hoffmann L, Møller DS, Knap MM, Rasmussen TR, et al. Systematic intrafraction shifts of mediastinal lymph node targets between setup imaging and radiation treatment delivery in lung cancer patients. Radiother Oncol 2018;126:318–24.
[43] Guckenberger M, Meyer J, Wilbert J, Richter A, Baier K, et al. Intra-fractional uncertainties in cone-beam CT based image-guided radiotherapy (IGRT) of pulmonary tumors. Radiother Oncol 2007;83:57–64.
[44] von Siebenthal M, Székely G, Lomax AJ, Cattin PC. Systematic errors in respiratory gating due to intrafraction deformations of the liver. Med Phys 2007;34:3620–9.
[45] Poulsen PR, Worm ES, Hansen R, Larsen LP, Grau C, Høyer M. Respiratory gating based on internal electromagnetic motion monitoring during stereotactic liver radiation therapy: first results. Acta Oncol 2015;54:1445–52.
[46] Worm ES, Høyer M, Fledelius W, Hansen AT, Poulsen PR. Variations in magnitude and directionality of respiratory target motion throughout full treatment courses of stereotactic body radiotherapy for tumors in the liver. Acta Oncol 2013;52:1437–44.
[47] Palmer J, Yang J, Pan T, Court LE. Motion of the esophagus due to cardiac motion. PLoS ONE 2014;9:e89126.
[48] Seppenwoolde Y, Shirato H, Kitamura K, Shimizu S, van Herk M, Lebesque JV, et al. Precise and real-time measurement of 3D tumor motion in lung due to breathing and heartbeat, measured during radiotherapy. Int J Radiat Oncol Biol Phys 2002;53:822–34.